

## Material Study on Reactively Sputtered Zinc Oxide for Thin Film Silicon Solar Cells

J. Hüpkens<sup>1</sup>, B. Rech<sup>1</sup>, S. Calnan<sup>1</sup>, O. Kluth<sup>1</sup>, U. Zastrow<sup>1</sup>, H. Siekmann<sup>1</sup>, M. Wuttig<sup>2</sup>

<sup>1</sup> Institute of Photovoltaics (IPV), Forschungszentrum Jülich GmbH, Jülich, Germany

<sup>2</sup> Institute for Physics of New Materials - Department of Physics, RWTH, Aachen, Germany

### Abstract

Aluminum doped zinc oxide films were prepared by reactive mid frequency magnetron sputtering. We characterized the electrical and optical properties as well as the surface morphology obtained after wet chemical etching. The carrier mobility could be increased up to 42 cm<sup>2</sup>/Vs and the transmission between 400 nm and 1100 nm was enhanced by the reduction of aluminum content in the targets. The working point of the reactive sputtering process strongly influences the etching behavior and was used to optimize the light scattering properties of the ZnO:Al films after wet chemical etching. Finally, the texture etched films were successfully applied as substrates for silicon thin film solar cells.

Keywords: zinc oxide (ZnO:Al), reactive sputtering, etching, thin film silicon, solar cells

### 1. Introduction

Silicon thin-film solar cells in the p-i-n (superstrate) structure require a transparent conductive oxide (TCO) film, which has to combine low series resistance and high transparency in the visible (400-800 nm) and, for microcrystalline silicon ( $\mu\text{c-Si:H}$ ), also in the near infra red (NIR) spectral range (up to 1100 nm). An adapted surface texture is required to provide light scattering and subsequent light trapping inside the silicon solar cell structure. Moreover, industrial applications need cost effective deposition techniques like the reactive mid frequency (mf) sputtering of aluminum doped zinc oxide (ZnO:Al) from metallic targets [1]. Sputtered ZnO:Al films are initially smooth in most cases, but develop different surface morphologies during a wet chemical etching step [2,3]. These texture etched films provide an efficient light trapping in silicon thin film solar cells and high solar cell efficiencies have been achieved for rf-sputtered ZnO:Al films from ceramic targets [4]. Also reactively mf-sputtered and texture etched ZnO:Al films have been successfully applied as substrates for large area amorphous silicon (a-Si:H) solar cells [5]. However, the light scattering properties and NIR transmission of the films have to be further improved with respect to the application in  $\mu\text{c-Si:H}$  solar cells to achieve high solar cell efficiencies. High transparency in the visible and NIR wavelength range combined with low resistivity requires high carrier mobilities [6], which can be experimentally realized for sputtered ZnO:Al-films by optimizing the aluminum doping concentration [7,8]. Earlier works studied the surface morphology after etching depending on the deposition conditions and revealed a strong influence of the deposition pressure [3,9] and the position on the substrate for statically deposited films [10].

This paper addresses the development of highly conductive and transparent ZnO:Al films by reactive mf-sputtering on 30x30 cm<sup>2</sup> substrate area. In view of an application as front contacts in silicon based thin film solar cells, we focused on the relationship between sputter parameters and the resulting film properties. First, we optimized the films by using different aluminum contents in the targets and varied the deposition parameters. Then we investigated the influence of the working point applied for the reactive sputtering process on the film properties. We studied the electrical and optical properties as well as the etching behavior, which is of crucial importance for the performance of silicon thin film solar cells. Finally, surface textured ZnO:Al films with suitable light scattering properties were applied as substrates for  $\mu\text{c-Si:H}$  based thin-film solar cells and modules.

## 2. Experiments

All ZnO:Al films were prepared on Corning (1737) glass substrates in an in-line sputtering system for a substrate size of 30x30 cm<sup>2</sup> (VISS 300, supplied by von Ardenne Anlagentechnik GmbH, Dresden, Germany). The sputtering system was operated in mf-sputtering mode using dual magnetron cathodes with metallic Zn:Al targets. The aluminum content was varied in steps between 0.2 wt% and 2 wt%. During the reactive sputtering process, the oxygen gas flow was controlled by plasma emission monitoring (PEM) [11]. The intensity of the 307 nm Zn emission line was used to characterize the process. The substrate oscillated in front of the cathodes to achieve adequate film thickness, typically between 700 nm and 900 nm. The thickness was measured using a surface profiler (Dektak 3030 by Veeco Instruments Inc.). The electrical film properties were investigated by four-point probe and room temperature Hall effect measurements, using a Keithley 926 Hall setup. Optical transmission of the ZnO:Al coated glass was measured with a dual beam spectrometer (Perkin Elmer, Lambda 19). To study the effect of doping, the aluminum content in the ZnO:Al films was determined by secondary ion mass spectrometry (SIMS). All values for Al film concentrations are given as Al/(Zn+Al) ratio. The error is less than 10 % relative. After deposition the initially smooth films were etched in diluted hydrochloric acid (0.5 % HCl) at room temperature or potassium hydroxide (33 % KOH) at 50 °C. The resulting surface morphology was characterized by scanning electron microscopy (SEM). Finally, mf-sputtered and texture-etched ZnO:Al films were applied as substrates for a-Si:H and  $\mu\text{c-Si:H}$  based p-i-n solar cells and modules. Details of silicon deposition by PECVD and the module preparation are described elsewhere (see [4,12] and references therein). Solar cell and module characterization was performed with a Wacom solar-simulator under standard test conditions (AM1.5, 100 mW/cm<sup>2</sup>, 25 °C).

## 3. Results

### 3.1 Stabilization of the reactive sputtering process

The reactive sputtering process has to be controlled in order to prepare high quality films, with high deposition rates, in the transition mode [1]. In our case, a plasma emission monitor (PEM) was used to control the oxygen flow during the reactive process [11]. Fig. 1 shows the hysteresis (dotted line) and the stabilized S-curve (solid line) of the generator voltage and the PEM intensity as a function of the oxygen flow measured with fixed discharge power. The process behavior with and without stabilization is described in detail

in [1,11]. The variations of PEM intensity are very similar to the variations of the discharge voltage, which is about a factor of two higher than the presented generator voltage. The process shows two stable modes, the metallic and the oxide mode. In the metallic mode, the generator voltage is about 350 V and the PEM intensity was calibrated to a value of 50. After the transition to the oxide mode, the values drop to about 220 V and less than 10, respectively. Using the PEM intensity to control the oxygen flow, an S-shaped curve can be observed in the transition mode. Every point on the S-curve represents a stabilized working point, where films can be prepared. The corresponding oxygen flow and PEM intensity do not depend on the target's history. The solid circles represent preparation conditions applied for investigated films. The PEM intensity is a relative value and the intensity values for different process conditions cannot be directly compared. For this reason, we use the PEM intensity to sort films prepared at different process conditions and compare optimized films for each series of working points.

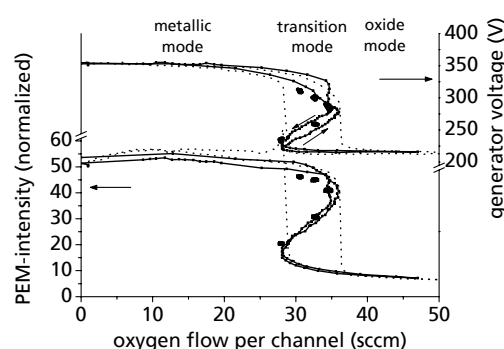


Fig. 1. Hysteresis and stabilization of the reactive sputtering process. The graph shows the PEM-intensity and generator voltage as a function of the oxygen flow for flow controlled mode (dotted line), stabilized mode (solid line) and deposited films (solid circles).

### 3.2 Study of substrate temperature and Al concentration

A systematic variation of the substrate temperature was performed by varying the heater temperature at a fixed deposition pressure for different Zn:Al alloy targets. The corresponding substrate temperature is about two thirds of the heater temperature. At each heater temperature, a variation of the working point was necessary to achieve the lowest resistivity. Fig. 2 shows the resistivity  $\rho$  as a function of the heater temperature for different targets. At room temperature, the lowest resistivity was in the range of  $30\text{-}90 \cdot 10^{-4}$  Ohmcm for all targets. With an aluminum concentration of 2 wt% in the target, a minimum resistivity was observed at a heater temperature of 350 °C. Towards higher temperatures,  $\rho$  increased to  $9 \cdot 10^{-4}$  Ohmcm at a heater temperature of  $T_H=420$  °C. Films prepared from targets with 1 wt% and 0.5 wt% show a very flat minimum of the resistivity at a heater temperature of 375 °C and 450 °C, respectively. For the lowest doping concentration, the resistivity decreases strongly up to a heater temperature of 500 °C, which was the highest applied in this study.

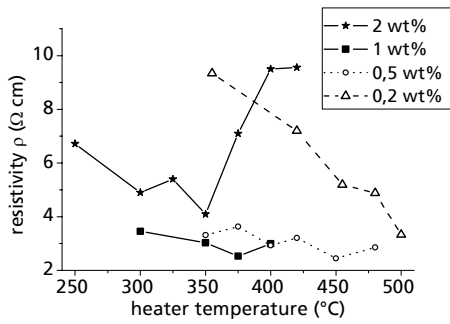


Fig. 2. Resistivity  $\rho$  of ZnO:Al films as a function of the heater temperature. The different curves correspond to films prepared from targets with different aluminum content given in the legend.

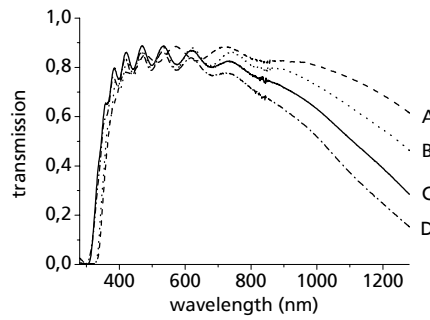


Fig. 3. Spectral transmission of ZnO:Al for targets with different Al concentrations using optimized sputtering conditions. Some film properties are given in Table 1.

Table 1

Thickness, aluminum concentration, resistivity  $\rho$ , carrier concentration  $N$  and mobility  $\mu$  of ZnO:Al-films shown in Fig. 3 and Fig. 6.

Film	Thickness (nm)	Al-concentration (at%)	$\rho$ ( $10^{-4}$ Ohmcm)	$N$ ( $10^{20}$ cm $^{-3}$ )	$\mu$ (cm $^2$ /Vs)
A	620	2.3	3.3	4.4	42
B	870	2.7	2.8	5.3	41
C	896	3.8	2.6	8.0	30
D	866	6.0	5.2	9.	13
E	906	1.1	17630	0.12	0.3
F	809	Not available	4.4	3.4	42
G	793	3.0	2.4	6.8	38

Fig. 3 shows the spectral transmission of electrically optimized films sputtered from different targets. The electrical properties and the thickness of the films are shown in Table 1. The differences in the film thickness even for film A, with a thickness of 620 nm, cannot explain the observed changes. According to the Burstein-Moss effect, the optical band gap shifts with the carrier concentration  $N$ . Between 400 nm and 600 nm, all films show very high transmission. The differences above 600 nm can be attributed to free carrier absorption resulting in lower transmission for highly doped films [6]. The lower aluminum concentration in the targets and in the corresponding films significantly improves the transmission in the NIR. The lower carrier concentration is compensated by the higher carrier mobility, which maintains the low resistivity.

Former studies on the influence of different doping concentrations on the film properties show enhanced mobilities for low doping concentrations [7]. Fig. 4 shows the carrier

concentration (Fig. 4a) and carrier mobility (Fig. 4b) as a function of the aluminum concentration in the films for the various preparation conditions. By increasing the Al concentration in the films, from 0.5 at% to 4 at%, the carrier concentration increased linearly up to  $8 \cdot 10^{20} \text{ cm}^{-3}$ . The incorporation of additional aluminum did not increase the carrier concentration further. The best carrier mobility of  $42 \text{ cm}^2/\text{Vs}$  was achieved for the low-doped films in the range between 2 at% and 3 at% (see Fig. 4b) prepared from the targets with 0.2 wt% or 0.5 wt% aluminum. At higher doping levels, the carrier mobility drops down to  $11 \text{ cm}^2/\text{Vs}$ . Note, that aluminum concentrations less than 1.5 at% were obtained at suboptimal preparation conditions explaining the rather poor mobilities. The lowest resistivity (not shown here) was observed for Al-concentrations between 3 at% and 4 at%.

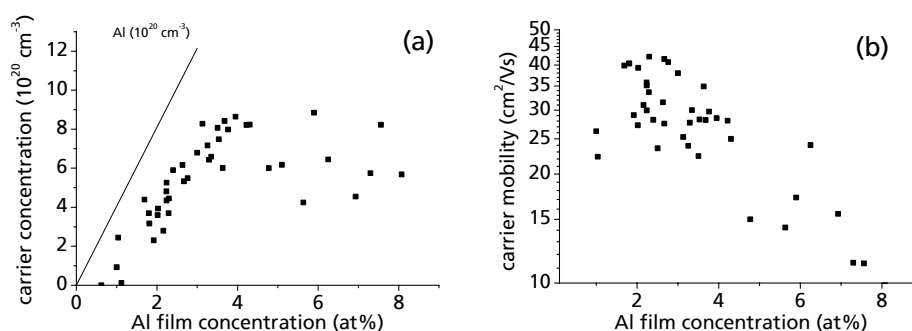


Fig. 4. Carrier concentration (a) and mobility (b) of the ZnO:Al films as a function of Al film concentration.

The best film properties regarding NIR transmission and the required sheet resistance for application in solar cells were achieved for the target with 0.2 % Al content at a heater temperature of  $500 \text{ }^\circ\text{C}$ . Due to practical reasons, the targets with Al concentration of 0.5 % and a heater temperature of  $420 \text{ }^\circ\text{C}$  were chosen for further studies on the working point and discharge power.

### 3.3 Influence of the working point on the optical and electrical properties

We prepared films at a total pressure of  $0.9 \text{ Pa}$  at different working points to study the effect on the film properties. Additionally, we increased the discharge power to enhance the deposition rate. Fig. 5a shows the deposition rate as a function of the PEM intensity achieved at different discharge power levels. Starting from the oxide mode the deposition rate increases and shows a maximum in the transition mode then decreases linearly towards the metallic mode. The maximum deposition rate linearly increases with the discharge power from  $47 \text{ nm}^*\text{m}/\text{min}$  to  $96 \text{ nm}^*\text{m}/\text{min}$  and  $115 \text{ nm}^*\text{m}/\text{min}$  for  $4 \text{ kW}$ ,  $8 \text{ kW}$  and  $10 \text{ kW}$ , respectively.

The electrical properties are plotted as a function of the PEM intensity in Fig. 5. The resistivity  $\rho$  (Fig. 5b) is high (up to  $1 \text{ Ohmcm}$ ) for films prepared in oxide mode and decreases to less than  $3 \cdot 10^{-4} \text{ Ohmcm}$  for working points close to the metallic mode. The carrier concentration (Fig. 5c) increases linearly with the PEM intensity for all discharge

powers from  $1 \cdot 10^{19} / \text{cm}^3$ , in the oxide mode, up to  $7 \cdot 10^{20} / \text{cm}^3$  in the metallic mode. The mobility  $\mu$  (Fig. 5d) shows a maximum of more than  $40 \text{ cm}^2/\text{Vs}$  in the transition mode.

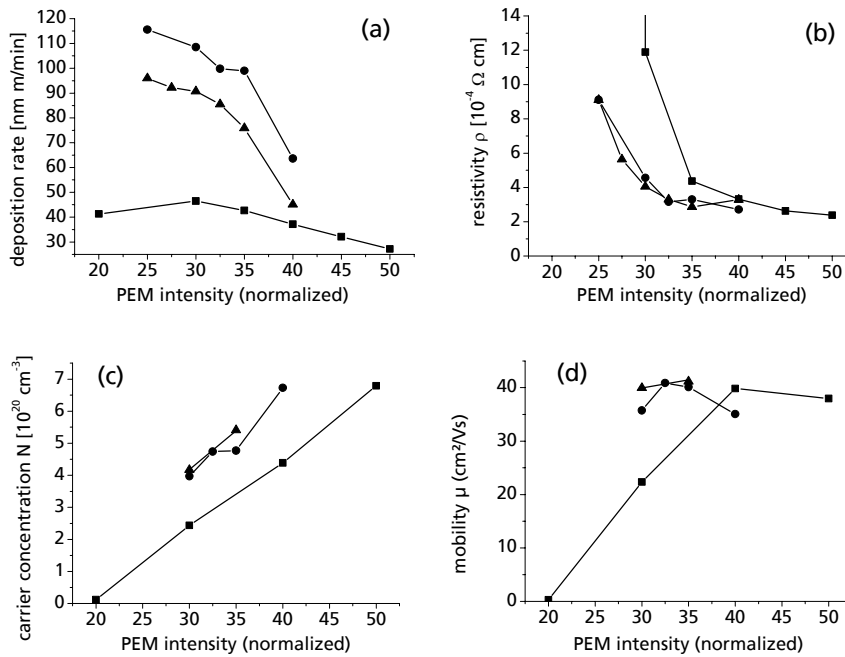


Fig. 5: Deposition rate (a) and electrical properties, resistivity (b), carrier concentration (c) and carrier mobility (d), for different discharge powers (squares (-■-) 4 kW, triangles (-▲-) 8 kW, circles (-●-) 10 kW) as a function of PEM-intensity, specifying the working point. The resistivity was measured by 4-point probe, the carrier concentration and mobility by Hall effect measurements.

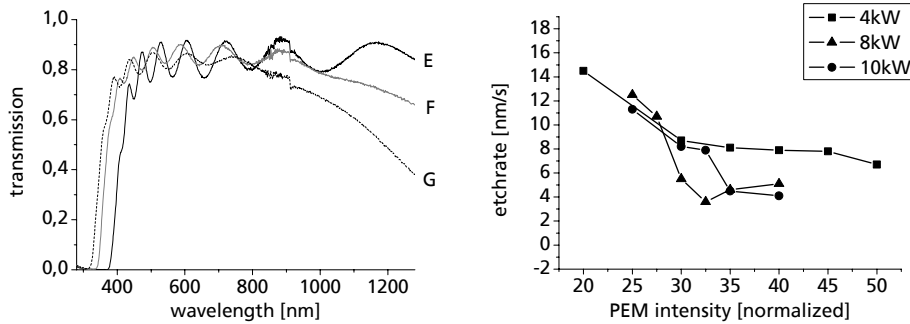


Fig. 6. Transmission of ZnO:Al coated glass for films from targets with different Aluminum content. The electrical properties of the films are shown in Table 1.

Fig. 7. Etch rates for films prepared at different discharge powers as a function of PEM intensity characterizing the working point. The films were etched for 30 to 40 seconds in HCl.

The different carrier concentrations for the different working points also influence the optical properties of the ZnO:Al films. Fig. 6 shows the spectral transmission for films prepared at different working points. The film thickness, aluminum concentration and electrical properties are given in Table 1. The different carrier concentrations affect the optical band gap and the transmission in the NIR. Film E shows the highest transmission in the NIR but its conductivity is not sufficient for the application in solar cells.

### 3.4 Surface textured films and application in solar cells

For application in thin film silicon solar cells, the initially smooth films had to be etched to obtain a rough, light scattering surface. In the following, we focus on the relationship between the working point (PEM intensity) of the sputter process and the resulting surface texture obtained after the etching step. Fig. 7 shows the etch rate determined after dipping the films for 30-40 seconds in diluted HCl. The etch rate of the films is high ( $>10$  nm/sec) for low PEM intensities close to the oxide mode and decreases approaching the metallic mode to an almost constant level. The lowest etch rate is 7-8 nm/sec for 4 kW and 4-5 nm/sec for the high power levels.

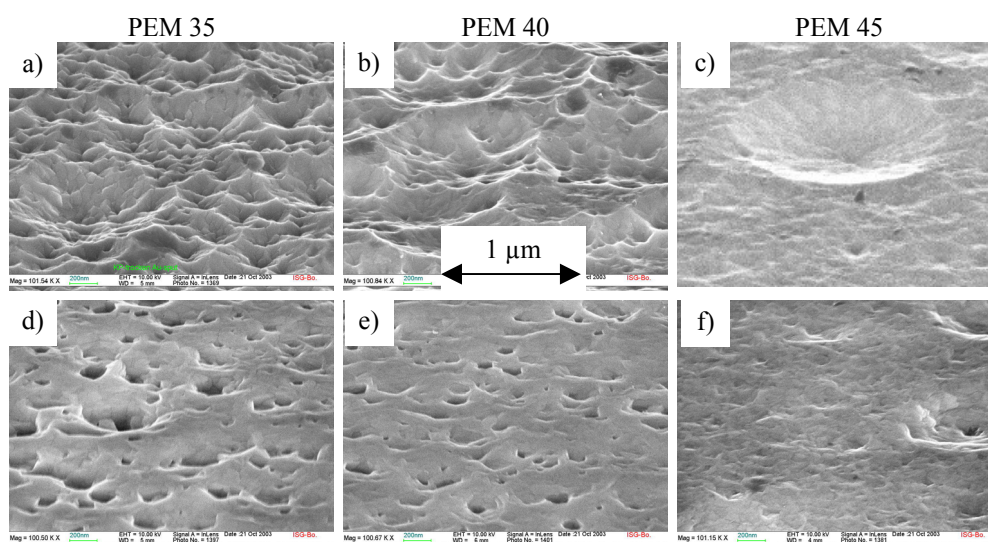


Fig. 8. SEM micrographs of texture-etched films prepared at different working points corresponding to PEM intensity 35 (left), 40 (middle) and 45 (right). The films a), b), and c) were etched in 0.5 % HCl; d), e) and f) were etched in 33 % KOH.

We further compared the influence of the working point on the surface morphology after etching either in 0.5% hydrochloric acid (at room temperature) or 33% potassium hydroxide (at 50°C). SEM images of selected films are shown in Fig. 8. The working point was varied in the transition mode from PEM intensity 35 on the left to 45 on the right. The films etched with HCl (Fig. 8a,b,c) had craters with sloping sides, while KOH (Fig. 8d,e,f) etched small holes vertically into the film. The surface between the etched holes appears to be not attacked by the KOH although the film thickness was reduced. For each etchant, the density of points of attack decreases as the working point approaches the metallic mode. The films prepared at PEM intensity of 35-40 and etched in HCl (Fig. 8a, b) show a regular

surface structure and high diffuse transmission making them promising candidates to provide efficient light trapping in silicon thin film solar cells.

Table 2

I/V-parameters (AM 1.5, 100 mW/cm<sup>2</sup>, 25 °C) of best solar cells and small area modules on texture etched MF sputtered ZnO:Al films. The substrate size was 10\*10 cm<sup>2</sup> for both the cells and modules.

Cell type	Cell or module	$\eta$ (%)	FF (%)	V <sub>OC</sub> (V)	I <sub>SC</sub> (mA)
a-Si:H	1 cm <sup>2</sup> Cell	10.1	69.2	0.90	16.3
$\mu$ c-Si:H	1 cm <sup>2</sup> Cell	8.2	71.2	0.51	22.4
a-Si:H/ $\mu$ c-Si:H	64 cm <sup>2</sup> module	9.7	69.0	10.6	85

Optimized films were applied after surface-texturing as front contacts for silicon thin film solar cells and mini modules (aperture area 64 cm<sup>2</sup>). Table 2 shows the I/V-parameters of the solar cells and modules measured under illumination. The best cell efficiencies for a-Si:H and  $\mu$ c-Si:H solar cells were 10.1 % and 8.2 %, respectively. A small area module incorporating an a-Si:H/ $\mu$ c-Si:H tandem cell showed an initial aperture area efficiency of 9.7 %.

#### 4. Discussion

The goal of this work was to study and develop textured ZnO:Al films for the application as textured front contacts for  $\mu$ c-Si:H based thin film solar cells. The requirements for such films are low resistivity, high transparency in the wavelength range between 400 nm and 1100 nm and an adapted surface structure to provide efficient light trapping. The reactive sputtering process from metallic targets was applied to be compatible with the cost requirements for industrial processes. From our experimental results we conclude, that for high transparency up to the NIR one has to apply low or moderate aluminum doping concentrations. In this case the substrate temperature has to be increased to improve the carrier mobility and to maintain low resistivities. The etching behavior and the resulting surface morphology strongly depend on the deposition conditions. Different etching behavior was observed in earlier works by variation of the deposition parameters like substrate temperature and deposition pressure [3,9] as well as the position on the substrate for statically deposited films [10]. In this work we demonstrate, that the working point of the reactive sputter deposition plays an important role for the density of points of attack during the etching step and thus also strongly influences the surface morphology obtained afterwards. In general, a microscopic model to describe the anisotropic etching of polycrystalline ZnO:Al films does not exist. Further work would be extremely helpful for the development of an optimized TCO for thin film silicon solar cells.

#### 5. Conclusion

ZnO:Al films with high conductivity and excellent transparency in the visible and also NIR were developed at high dynamic deposition rates of up to 115 nm<sup>3</sup>/min by mid frequency

magnetron sputtering. An optimization of the aluminum concentration and the substrate temperature leads to high carrier mobility of  $42 \text{ cm}^2/\text{Vs}$ . Upon wet chemical etching, the films developed different surface morphologies, which depends on the initial film properties. The etching behavior was strongly affected by the working point applied for the sputtering process. We propose, that within certain limits, the variation of the working point can be used as tool to optimize reactively sputtered ZnO:Al films for application in silicon thin film solar cells. Solar cells and small area modules were prepared on ZnO:Al films with good electrical, optical and light scattering properties. An initial aperture area module efficiency of 9.7 % for an a-Si:H/ $\mu\text{c-Si:H}$  tandem module demonstrates the potential of this approach.

### Acknowledgments

The authors thank H. P. Bochem for SEM-measurements and B. Sehrbrock, J. Kirchhoff, C. Zahren and W. Appenzeller for technical assistance. We thank J. Müller, B. Szyszka, F. Ruske and V. Sittinger for many fruitful discussions. We gratefully acknowledge financial support by the BMWi (contract No. 0329923A).

### References

- [1] B. Szyszka, *Thin Solid Films* 351 (1999) 164-169
- [2] Löffl, S. Wieder, B. Rech, O. Kluth, C. Beneking, and H. Wagner, *Proceedings of the 14th European Solar Energy Conference, Barcelona* p. 2089 (1997)
- [3] O. Kluth, G. Schöpe, J. Hüpkes, C. Agashe, J. Müller, B. Rech, *Thin Solid Films* 442 (2003) 80–85
- [4] B. Rech, O. Kluth, T. Repmann, J. Springer, J. Müller, F. Finger, H. Stiebig, H. Wagner, *Solar Energy Materials and Solar Cells* 74 (2002) 439-447
- [5] J. Müller, G. Schöpe, O. Kluth, V. Sittinger, B. Szyszka, R. Geyer, P. Lechner, H. Schade, M. Ruske, G. Dittmar, H.-P. Bochem, *Thin Solid Films* 442 (2003) 158-162
- [6] K.L. Chopra, S. Major and D.K. Pandya, *Thin Solid Films* 102, 1 (1983)
- [7] T. Minami, H. Sato, H. Nanto, S. Takata, *Jap. Journal of Applied Physics* 24 10 (1985) 781-784
- [8] C. Agashe, O. Kluth, G. Schöpe, H. Siekmann, J. Hüpkes, B. Rech, *Thin Solid Films* 442, (2003) 167-172
- [9] J. Hüpkes, B. Rech, O. Kluth, T. Repmann, B. Sehrbrock, J. Müller, R. Drese, M. Wuttig, *Technical Digest of the 14th Int. Photovoltaic Science and Engineering Conference PVSEC-14, Bangkok, 2004, Vol. I, 379-380, submitted to Solar Energy Materials and Solar Cells*
- [10] J. Hüpkes, B. Rech, O. Kluth, J. Müller, H. Siekmann, C. Agashe, H.P. Bochem, M. Wuttig, *Materials Research Society Symposium Proceedings* 762, A7.11 (2003)
- [11] C. May, R. Menner, J. Strümpfel, M. Oertel, B. Sprecher, *Surface and Coatings Technology* 169-170 (2003) 512–516
- [12] B. Rech, J. Müller, T. Repmann, O. Kluth, T. Roschek, J. Hüpkes, H. Stiebig, W. Appenzeller, *Materials Research Society Symposium Proceedings* 762, A3.1 (2003)